Supplementary material

Pakizer D, Netuka D, Hrbáč T, et al. MRI- and CT-derived carotid plaque characteristics and stroke: Insights from the ANTIQUE study. Pol Heart J. 2024.

METHODS

Definitions of other diseases associated with carotid atherosclerosis

Definitions of ischemic cerebrovascular events are provided in the main manuscript. Definitions of all other comorbidities extracted from anamnestic patient data and included in our manuscript are listed below:

Arterial hypertension: systolic blood pressure ≥140 mm Hg and/or diastolic blood pressure ≥90 mm Hg [1].

Diabetes mellitus: a group of metabolic diseases characterized by hyperglycemia resulting from defects in insulin secretion, insulin action, or both [2].

Dyslipidemia: any abnormal levels of total cholesterol (≥200 mg/dl), low-density lipoprotein cholesterol (≥100 mg/dL), high-density lipoprotein cholesterol (>40 mg/dl for men or <50 mg/dL for women), non–high-density lipoprotein cholesterol (≤130 mg/dl), triglycerides (≤150 mg/dl), or taking lipid-lowering medication [3].

Coronary artery disease: a pathological process characterized by atherosclerotic plaque accumulation in the epicardial arteries, whether obstructive or non-obstructive [4].

Myocardial infarction: post-interventional cardiac troponin T level increase of >2 times the normal upper limit in addition to either chest pain, symptoms consistent with heart ischemia, or electrocardiographic evidence of ischemia [5].

Atrial fibrillation: rapid, disorganized atrial electrical activation leading to ineffective atrial contraction, characterized by electrocardiographic characteristics such as absence of distinct P waves on the surface ECG; irregular atrial activations with an atrial cycle length that is usually <200 ms; and ‘absolutely’ irregular R–R intervals (when atrioventricular conduction is not impaired) [6].

Chronic kidney disease: the presence of kidney damage or an estimated glomerular filtration rate of less than 60 ml/min/1.73 m^2, persisting for 3 months or more, irrespective of cause [7].

Autoimmune disease: humoral or cell-mediated immune response to self-antigen [8].

Hemorrhagic stroke: rapidly developing clinical signs of neurological dysfunction attributable to a focal collection of blood within the brain parenchyma or ventricular system that is not caused by trauma [9].

Computed tomography

All patients underwent standard helical multidetector computed tomography angiography (CTA) of the cerebral and carotid arteries with Siemens Somatom Definition AS, Definition AS+, Definition Edge, Emotion 16 and Perspective (Siemens Healthineers, Erlangen, Germany); Toshiba Aquilion 16, 64 and Prime (Canon Medical Systems Corporation, Otawara, Japan); Phillips Brilliance 6, Brilliance iCT 128 and Ingeunity Core 128 (Koninklijke Philips Electronics N.V., Amsterdam, The Netherlands); and GE Healthcare BrightSpeed Elite and Optima CT660 (General Electric Healthcare, Chicago, USA) devices. All examinations were performed with 50–100 ml of the intravenous iodine contrast agents (CA), Iomeron® 400 (Bracco Imaging, Milan, Italy) or Ultravist® 370 (Bayer HealthCare Pharmaceuticals LLC, Berlin, Germany), depending on scan duration and patient weight. Contrast agents were administered at a rate of 3–4 ml/s with an automatic injector through a minimum 20 G cannula inserted into a peripheral vein. The arterial phase of the examination was triggered by bolus tracking in the ascending aorta. Each patient was examined in supine position, and the scanning direction was caudocranial. The CT scan ranged from the lower edge of the aortic arch to the vertex of the skull (above the Willis circle). Multiplanar reconstructions in the axial plane in submillimeter sections and reconstructions of maximum intensity projection in the sagittal and coronal planes in 3–8 mm sections, with a uniform window width (W) of 700 Hounsfield units (HU) and window center (L) of 200 HU, were assessed. In several cases, the width and center of the window needed to be increased for optimal visualization (range W 700–1000 HU and L 200–400 HU).

Magnetic resonance imaging

Magnetic resonance imaging (MRI) examinations of carotid arteries were performed on Siemens Avanto 1.5 T and Skyra 3 T (Siemens Healthineers, Erlangen, Germany), GE Healthcare Discovery MR750w 3 T (General Electric Healthcare, Chicago, IL, US) and Philips Ingenia 3 T (Koninklijke Philips Electronics NV, Amsterdam, Netherlands) instruments. The receiving coil comprised a head/neck angiographic or cervical multichannel coil. The field of view was centered on stenosis in the carotid bifurcation.

The MRI carotid bifurcation examination protocol consisted of four basic sequences:

1. T1-weighted_TSE (turbo spin echo)_FS (fat suppressed) sequence, axial planes (time to echo [TE] 19 ms, time to repeat [TR] 600 ms; slice thickness [ST] 3 mm; matrix size 230 × 256; distance factor [gap] 0.3 mm; field of view [FOV] 256 mm; FOV phase 100%; turbo factor [TF] 2; number of excitations [NEX] 2; sequence length 3:50 min).
2. 3D_T1_MPRAGE (magnetization prepared rapid gradient echo) sequence, axial planes, IPH sensitive (TE 4 ms; TR 670 ms; TI 370 ms, ST 1 mm; matrix size 192 × 256; gap 0 mm; FOV 180 mm; FOV phase 75; Q3 NEX 3; sequence length 5:49 min).
3. T2-weighted TSE sequence, axial planes (TE 72 ms; TR 4 580 ms; ST 4 mm; matrix size 294 × 384; gap 0.4 mm; FOV 230 mm; FOV phase 100, TF 14; Q3 NEX 2; sequence length 3:18 min).
4. 3D_TOF (time of flight) sequence, axial planes (TE 7 ms; TR 24 ms; ST 1 mm; matrix size, 198 × 384; gap 0 mm; FOV 200 mm; FOV phase 75%; Q3 NEX 1; sequence length 2:43 min).

In selected patients, MRI carotid artery examination was performed with CA, administered in the second part of the examination. Either 7.5–10 ml gadolinium CA Gadovist® (Bayer HealthCare Pharmaceuticals LLC, Berlin, Germany) or 10 ml MultiHance® (Bracco Imaging, Milan, Italy) was administered intravenously. The post-contrast acquisition was T1-weighted TSE with fat suppression.

The degree of stenosis was measured according to the NASCET criteria [10] specifically on TOF sequences. The general plaque composition was evaluated according to the modified American Heart Association (AHA) classification for MRI in four categories: type IV–V: plaque with a lipid-rich necrotic core (LRNC) surrounded by fibrous tissue with possible calcification; type VI: complex plaque with possible surface defects, hemorrhage or thrombi; type VII: calcified plaque; and type VIII: fibrotic plaque without LRNC with possible small calcifications [11]. LRNC appeared as isointense on TOF images, isointense to hyperintense on T1w, and hypointense on T2w images; fibrous tissue as isointense on TOF images and isointense to hyperintense on T1w and T2w images; and calcification nodules as hypointense areas in all images (T1w, T2w, and TOF) [12]. In patients examined by MRI with a CA, enhancement as a marker of plaque neovascularization and inflammation was evaluated on postcontrast T1w sequences (increased enhancement with CA: hyperintensity compared to the same sequence before admission of CA) [13, 14].

RESULTS

In the beginning, the following variables were included in the logistic regression analysis, step 1: age of patients, male sex, coronary arterial disease, lipid part on CT, overall AHA type, AHA type IV–V,

AHA type VI, AHA type VII, stenosis degree on MRI, alcohol, and smoking. Variables with the highest significance value were gradually removed from the model (backward elimination – starts with a set of independent variables, deleting one at a time, then testing to see if the removed variable is statistically significant). Finally, the model consisted of 9 steps. Detailed results of the logistic regression analysis are provided in *Table S1*. The final model included only alcohol and stenosis severity on which results are provided in the main manuscript.

Table S1. Logistic regression using backward stepwise (likelihood ratio) method

		Coefficient	**Standard error**	**Wald**	**Degrees of freedom**	***P*-value**	**Odds ratio**	**95% confidence interval for odds ratio**	
								Lower	**Upper**
Step 1[a]	Age of patients	0.008	0.023	0.124	1	0.724	1.008	0.963	1.055
	Male sex	–0.077	0.457	0.028	1	0.867	0.926	0.378	2.267
	Coronary arterial disease	–0.457	0.454	1.012	1	0.315	0.633	0.260	1.542
	Lipid part on CT	0.523	0.755	0.479	1	0.489	1.687	0.384	7.415
	Overall AHA type			2.256	3	0.521			
	AHA type IV–V	–0.468	0.465	1.015	1	0.314	0.626	0.252	1.557

	AHA type VI	–0.657	0.842	0.609	1	0.435	0.518	0.099	2.701
	AHA type VII	–1.011	0.768	1.733	1	0.188	0.364	0.081	1.640
	Stenosis degree on MRI	0.032	0.012	7.027	1	0.008	1.032	1.008	1.056
	Alcohol	1.146	0.420	7.458	1	0.006	3.147	1.382	7.165
	Smoking	0.559	0.399	1.960	1	0.162	1.749	0.800	3.824
	Constant	–4.368	1.943	5.055	1	0.025	0.013		
Step 2[a]	Age of patients	0.007	0.023	0.098	1	0.755	1.007	0.962	1.054
	Male sex	–0.121	0.448	0.073	1	0.788	0.886	0.368	2.134
	Coronary arterial disease	–0.450	0.452	0.991	1	0.320	0.638	0.263	1.546
	Lipid part on CT	0.452	0.737	0.376	1	0.540	1.571	0.370	6.664
	Overall AHA type			2.082	3	0.556			
	AHA type IV–V	–0.424	0.456	0.868	1	0.352	0.654	0.268	1.598
	AHA type VI	–0.461	0.717	0.414	1	0.520	0.631	0.155	2.569

	AHA type VII	–0.880	0.685	1.652	1	0.199	0.415	0.108	1.587
	Stenosis degree on MRI	0.031	0.012	6.999	1	0.008	1.031	1.008	1.055
	Alcohol	1.163	0.416	7.833	1	0.005	3.200	1.417	7.226
	Smoking	0.563	0.399	1.994	1	0.158	1.756	0.804	3.837
	Constant	–4.223	1.914	4.868	1	0.027	0.015		
Step 3[a]	Age of patients	0.007	0.023	0.100	1	0.752	1.007	0.963	1.054
	Coronary arterial disease	–0.452	0.451	1.003	1	0.317	0.636	0.263	1.541
	Lipid part on CT	0.445	0.737	0.364	1	0.546	1.560	0.368	6.608
	Overall AHA type			2.052	3	0.562			
	AHA type IV–V	–0.420	0.455	0.849	1	0.357	0.657	0.269	1.605
	AHA type VI	–0.460	0.716	0.413	1	0.521	0.631	0.155	2.567
	AHA type VII	–0.875	0.686	1.629	1	0.202	0.417	0.109	1.598

	Stenosis degree on MRI	0.030	0.011	6.983	1	0.008	1.031	1.008	1.054
	Alcohol	1.151	0.413	7.780	1	0.005	3.163	1.408	7.102
	Smoking	0.551	0.396	1.936	1	0.164	1.736	0.798	3.774
	Constant	–4.222	1.913	4.870	1	0.027	0.015		
Step 4[a]	Coronary arterial disease	–0.433	0.448	0.935	1	0.334	0.648	0.269	1.560
	Lipid part on CT	0.459	0.734	0.391	1	0.532	1.582	0.376	6.663
	Overall AHA type			2.046	3	0.563			
	AHA type IV–V	–0.420	0.456	0.851	1	0.356	0.657	0.269	1.604
	AHA type VI	–0.453	0.716	0.401	1	0.526	0.636	0.156	2.583
	AHA type VII	–0.872	0.685	1.623	1	0.203	0.418	0.109	1.600
	Stenosis degree on MRI	0.030	0.011	6.932	1	0.008	1.031	1.008	1.054
	Alcohol	1.160	0.412	7.920	1	0.005	3.189	1.422	7.152

	Smoking	0.530	0.390	1.843	1	0.175	1.698	0.791	3.648
	Constant	–3.688	0.872	17.898	1	0	0.025		
Step 5[a]	Coronary arterial disease	–0.417	0.442	0.888	1	0.346	0.659	0.277	1.568
	Lipid part on CT	0.681	0.633	1.157	1	0.282	1.976	0.571	6.833
	Stenosis degree on MRI	0.032	0.011	8.223	1	0.004	1.033	1.010	1.056
	Alcohol	1.178	0.389	9.148	1	0.002	3.247	1.514	6.967
	Smoking	0.540	0.386	1.959	1	0.162	1.715	0.806	3.652
	Constant	–3.775	0.868	18.897	1	0	0.023		
Step 6[a]	Lipid part on CT	0.682	0.633	1.160	1	0.281	1.978	0.572	6.844
	Stenosis degree on MRI	0.032	0.011	8.266	1	0.004	1.033	1.010	1.056
	Alcohol	1.168	0.388	9.081	1	0.003	3.216	1.504	6.877
	Smoking	0.567	0.383	2.195	1	0.138	1.763	0.833	3.734

	Constant	–3.768	0.871	18.697	1	0	0.023		
Step 7[a]	Lipid part on CT	0.719	0.635	1.284	1	0.257	2.053	0.592	7.124
	Stenosis degree on MRI	0.032	0.011	7.837	1	0.005	1.032	1.010	1.055
	Alcohol	1.194	0.386	9.565	1	0.002	3.300	1.548	7.032
	Smoking	0.551	0.381	2.088	1	0.148	1.735	0.822	3.664
	Constant	–3.628	0.864	17.642	1	0	0.027		
Step 8[a]	Stenosis degree on MRI	0.035	0.011	10.263	1	0.001	1.036	1.014	1.058
	Alcohol	1.227	0.384	10.198	1	0.001	3.413	1.607	7.249
	Smoking	0.579	0.380	2.326	1	0.127	1.784	0.848	3.756
	Constant	–3.599	0.859	17.542	1	0	0.027		
Step 9[a]	Stenosis degree on MRI	0.036	0.011	11.225	1	0.001	1.037	1.015	1.059
	Alcohol	1.273	0.380	11.196	1	0.001	3.571	1.694	7.527
	Constant	–3.758	0.844	19.823	1	0	0.023		

Abbreviations: AHA, American Heart Association; CT, computed tomography; MRI, magnetic resonance imaging

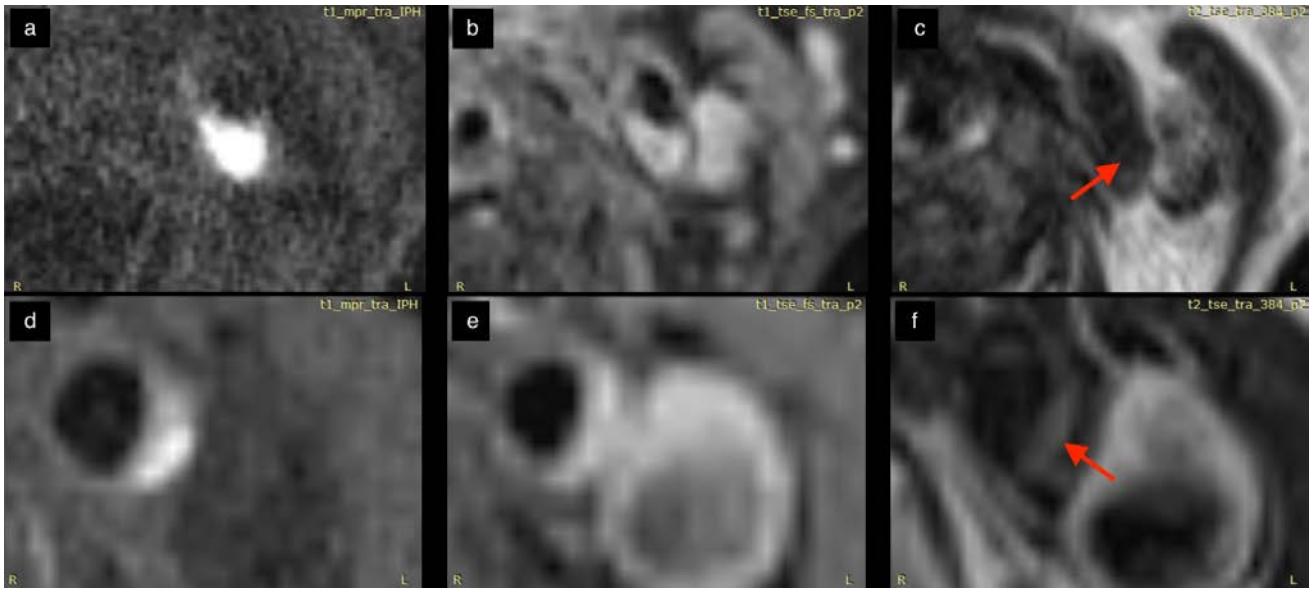

Figure S1. MRI detection of an intraplaque hemorrhage. Acute intraplaque hemorrhage (ICA sin., axial planes) located deep within the plaque appears as a hyperintense signal on T1w MPRAGE IPH sensitive (**a**) and T1w TSE FS (**b**) sequences, and hypointense signal on T2w TSE (**c**, arrow). Subacute intraplaque hemorrhage appears as a hyperintense signal on T1w MPRAGE IPH sensitive (**d**), T1w FSE FS (**e**), and T2w TSE (**f**, arrow) sequence

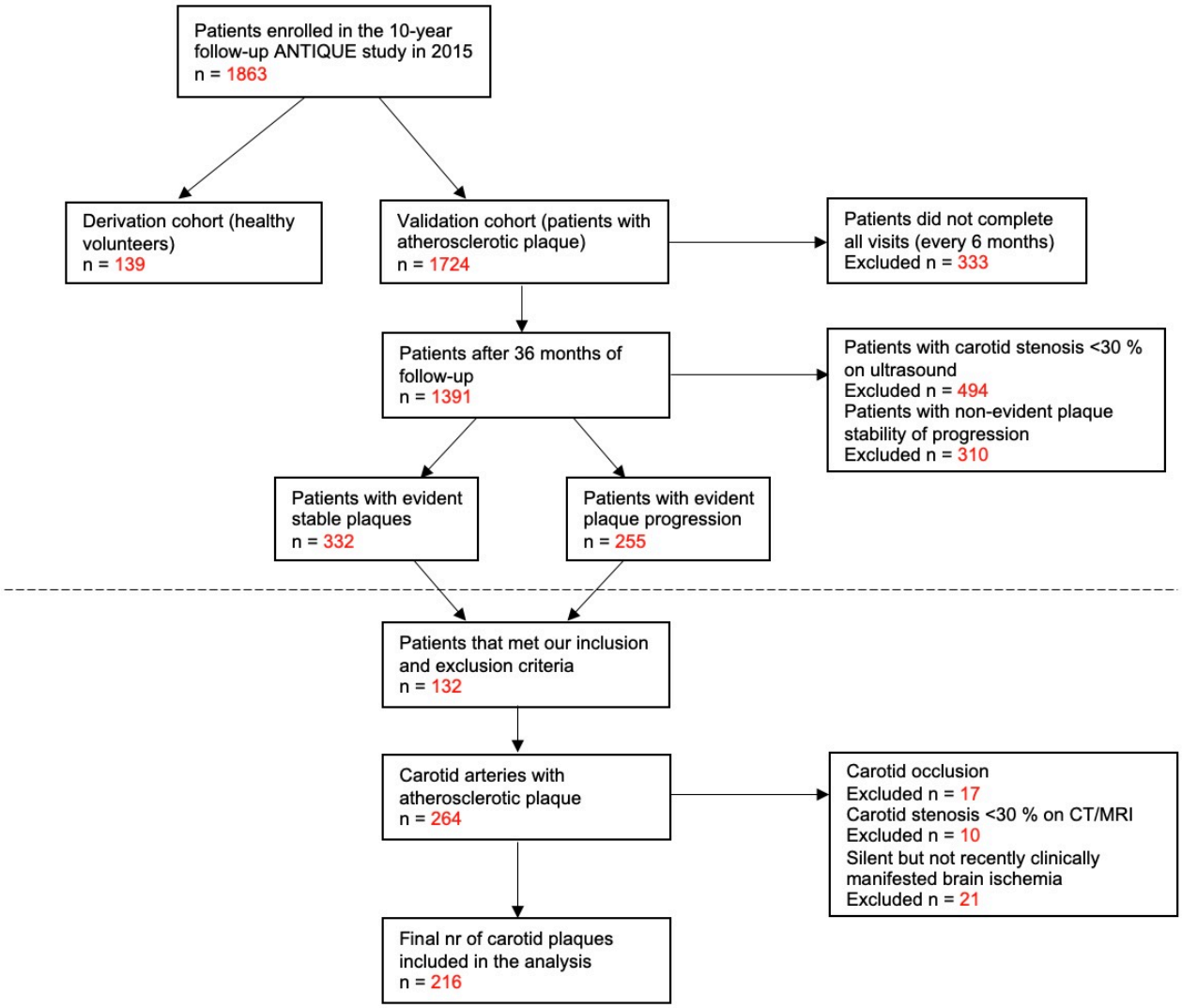

Figure S2. Study flow chart diagram

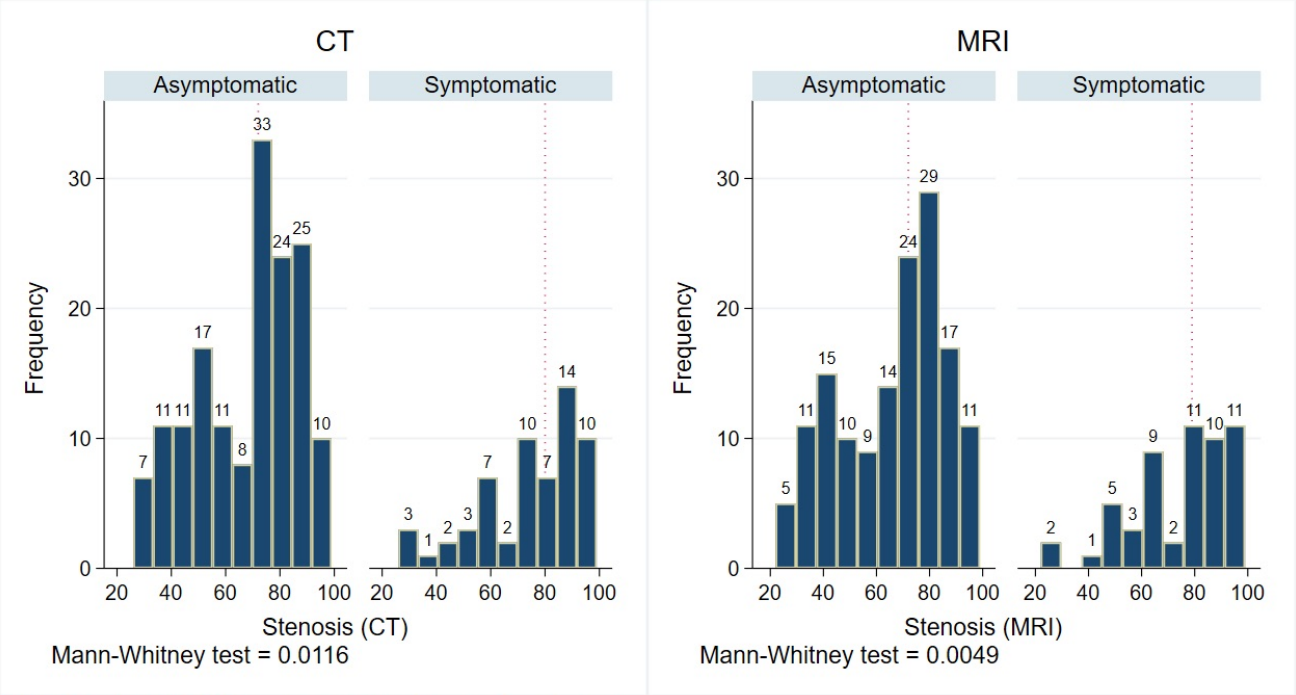

Figure S3. Distribution of carotid stenosis severity in symptomatic and asymptomatic stable plaques according to CT and MRI examinations

REFERENCES

1. Williams B, Mancia G, Spiering W, et al. 2018 ESC/ESH Guidelines for the management of arterial hypertension. Eur Heart J. 2018; 39(33): 3021–3104, doi: 10.1093/eurheartj/ehy339, indexed in Pubmed: 30165516.
2. American Diabetes Association. Diagnosis and classification of diabetes mellitus. Diabetes Care. 2010; 33(Suppl 1): S62–S69, doi: 10.2337/dc10-s062.
3. Di Angelantonio E, Sarwar N, Perry P, et al. Major lipids, apolipoproteins, and risk of vascular disease. JAMA. 2009; 302(18): 1993–2000, doi: 10.1001/jama.2009.1619, indexed in Pubmed: 19903920.
4. Knuuti J, Wijns W, Saraste A, et al. 2019 ESC Guidelines for the diagnosis and management of chronic coronary syndromes. Eur Heart J. 2020; 41(3): 407–477, doi: 10.1093/eurheartj/ehz425, indexed in Pubmed: 31504439.
5. Thygesen K, Alpert JS, White HD, et al. Third universal definition of myocardial infarction. Eur Heart J. 2012; 33(20): 2551–2567, doi: 10.1093/eurheartj/ehs184, indexed in Pubmed: 22922414.

6. Kirchhof P, Benussi S, Kotecha D, et al. 2016 ESC Guidelines for the management of atrial fibrillation developed in collaboration with EACTS. Eur Heart J. 2016; 37(38): 2893–2962, doi: 10.1093/eurheartj/ehw210, indexed in Pubmed: 27567408.
7. Levey AS, Eckardt KU, Tsukamoto Y, et al. Definition and classification of chronic kidney disease: A position statement from Kidney Disease: Improving Global Outcomes (KDIGO). Kidney Int. 2005; 67(6): 2089–2100, doi: 10.1111/j.1523-1755.2005.00365.x, indexed in Pubmed: 15882252.
8. Wang L, Wang FS, Gershwin ME. Human autoimmune diseases: A comprehensive update. J Intern Med. 2015; 278(4): 369–395, doi: 10.1111/joim.12395, indexed in Pubmed: 26212387.
9. Sacco R, Kasner S, Broderick J, et al. An updated definition of stroke for the 21st century. Stroke. 2013; 44(7): 2064–2089, doi: 10.1161/str.0b013e318296aeca.
10. Barnett HJM, Taylor DW, Haynes RB, et al. Beneficial effect of carotid endarterectomy in symptomatic patients with high-grade carotid stenosis. N Engl J Med. 1991; 325(7): 445–453, doi: 10.1056/NEJM199108153250701, indexed in Pubmed: 1852179.
11. Cai JM, Hatsukami TS, Ferguson MS, et al. Classification of human carotid atherosclerotic lesions with in vivo multicontrast magnetic resonance imaging. Circulation. 2002; 106(11): 1368–1373, doi: 10.1161/01.cir.0000028591.44554.f9, indexed in Pubmed: 12221054.
12. Saam T, Ferguson MS, Yarnykh VL, et al. Quantitative evaluation of carotid plaque composition by in vivo MRI. Arterioscler Thromb Vasc Biol. 2005; 25(1): 234–239, doi: 10.1161/01.ATV.0000149867.61851.31, indexed in Pubmed: 15528475.
13. Saba L, Saam T, Jäger HR, et al. Imaging biomarkers of vulnerable carotid plaques for stroke risk prediction and their potential clinical implications. Lancet Neurol. 2019; 18(6): 559–572, doi: 10.1016/S1474-4422(19)30035-3, indexed in Pubmed: 30954372.
14. Saba L, Yuan C, Hatsukami TS, et al. Carotid artery wall imaging: perspective and guidelines from the ASNR vessel wall imaging study group and expert consensus recommendations of the American Society of Neuroradiology. AJNR Am J Neuroradiol. 2018; 39(2): E9–E31, doi: 10.3174/ajnr.A5488, indexed in Pubmed: 29326139.